3.5 ARROW structures: Fabrication

During the first part of this chapter, an analysis of the most remarkable technological processes that could bring the fabrication of ARROW structures has been presented. The antiresonant layers of an ARROW-A structure can be obtained by thermal growth and LPCVD, assuring high-quality layers but with a fixed refractive index. Nevertheless, the core of the ARROW-A and the whole ARROW-B structure needs a layer deposition technique that allows selecting a concrete refractive index. Amorphous silicon oxide (a-SiO_x, $x<2$) obtained by PECVD has been chosen for the fabrication of the ARROW structures. The easiness of varying the refractive indexes of the layer deposited when the deposition conditions are modified, specially the precursor ratio ($R=[N_2O]/[SiH_4]$) and the deposition temperature T_d **[17]** is its major advantage. During deposition, different impurities such as hydrogen, nitrogen and water are incorporated to the a-SiO_x layer. Furthermore, moisture can be adsorbed from the atmosphere after deposition. The effect of these contaminants on the layer properties must be known beforehand, since its properties should be fixed and stable. Thus, in order to analyze if the selected internal and external asymmetry coefficients proposed could be obtained or not with PECVD, a complete characterization of the layers deposited with this technique must be done.

This study has been mainly focused on the effects that could cause a higher variation on the performance of integrated optics devices. Concerning the optical properties, the refractive index and the absorption coefficient are the most significant parameters that have to be controlled. Since deposition processes are done sequentially, it becomes necessary to study the effect of the temperature on the layers obtained. Moreover, the bonds of impurities act as absorption or scattering centers, causing a significant increase of the transmission losses. Then, it will be very useful, if possible, to have impurity-free films. This can be done by ways of the Rapid Thermal Annealing (RTA) system (ADAX-1000), which basically consists on a temperature trigger shot, that is, heating the sample fastly over a very short period of time that causes impurity effusion. For obtaining information concerning the film structural and compositional properties, FTIR layer spectra have been done. Normally, the vibrational modes of the

molecular species have resonant frequencies that fall into the IR range. Hence, using a broadband infrared light source and a monochromator, it is possible to scan the layer transmitted light (or the reflected, depending on the configuration used) as a function of the wavelength. This non-destructive analysis method provides with information concerning composition, amount of impurities, layer thickness and refractive index.

The deposition processes were done using a PLASMALAB 80+ radial flow capacitively coupled parallel-plate PECVD reactor, operated at 13.56 MHz. Chamber pressure, RF power density and substrate temperature during depositions were 26.6 Pa, 0.07 W/cm^2 and 200 ºC, respectively, except when the temperature effects were under study. The N_2O flow was fixed at 110sccm and R was varied between 2.2 and 55. Deposition processes were carried out on 50 mm diameter, one-side polished, p-type, 14-20Ω.cm, (100)-oriented, 290µm thick silicon wafers.

The first step done on the SiO_x characterization was to analyze how the layer thickness affects its optical properties. Two different sets of layers, with thicknesses of 0.1µm and 1µm were obtained. Refractive index was measured over 50 different sample points with a Rudolph Research Auto El IV ellipsometer working at 632.8 nm and 70º incidence angle. Averaged values were considered. Results are shown in fig. 3.17a. As can be seen, the refractive index for both thicknesses is nearly equal, being slightly different only in the very low R region. It can be observed the expected huge flexibility on having layers with different refractive index. Only by varying R, it has been possible to obtain refractive index values that range from these of the thermal silicon oxide to values close to the silicon nitride. This fact can be associated to the high Si-Si bond concentration on the layers. Afterwards, layers with a thickness of 1.0µm suffered from a RTA annealing at 950ºC during 30 seconds in an inert atmosphere. Results can be seen in fig. 3.17b. Two different regions can be defined: for very low R-values, refractive index sharply increases, probably due to the nano-cluster silicon formation. On the contrary, at medium R values ($10<R<25$) there is a slight decrease of the refractive index, that can be associated to impurity effusion maintaining the film porosity. Finally, at high R-values, no appreciable modification of the refractive index after RTA annealing is observed.

Measurements done by ellipsometric spectroscopy **[18]** have provided with information concerning the layer extinction coefficient (κ). As can be seen in fig. 3.17c, when the precursor ratio decreases, κ has a non-zero value at low wavelengths. Although our working wavelength will always be above 0.5μm, it is a factor that should be considered if waveguides with high refractive index (i.e., low R) where to be done, since the core material will inherently act as a wavelength high-pass filter.

From the previous results, first ARROW-A waveguides were obtained. The 2nd cladding layer was a 2μm thermally-obtained silicon oxide, the 1st cladding layer was a LPCVD-deposited silicon nitride and had a thickness of 0.38μm and the core consists on 4μm PECVD-deposited silicon oxide layer with R=7.5. Then, the rib was defined by RIE using CHF_3 as precursor at 500Watt and at a working pressure of 5.0Pa. These etching conditions provide with a silicon oxide etching speed of 1000Å/min. After a 2.5μm-deep etching, integrated optical devices were nearly done and only passivation of the structure need to be done. However, after a 2μm PECVD-deposited silicon oxide layer with R=40, the structure had an excessive mechanical stress and it cracked as shown in fig. 3.18. It is not necessary mentioning that these facts cause several drawbacks: **1. Irreversible structure cracking**, which means that none of the devices on the wafer would work. **2. Cost**: Since stress is additive, the layer that causes the structure to collapse is the last. Thence, all the investment necessary so as to obtain the multilayer stack is worthless. **3. Cleaning**: Generally, crack is produced during heating/cooling the sample (even at low temperatures) due to different mechanical coefficients between the layers. The layer breaks into small particles that are spread not only over the wafer, but also on the reactor and the wafer try, being necessary to disassemble and cleaning all the deposition system before doing a new process, which obviously is a major drawback.

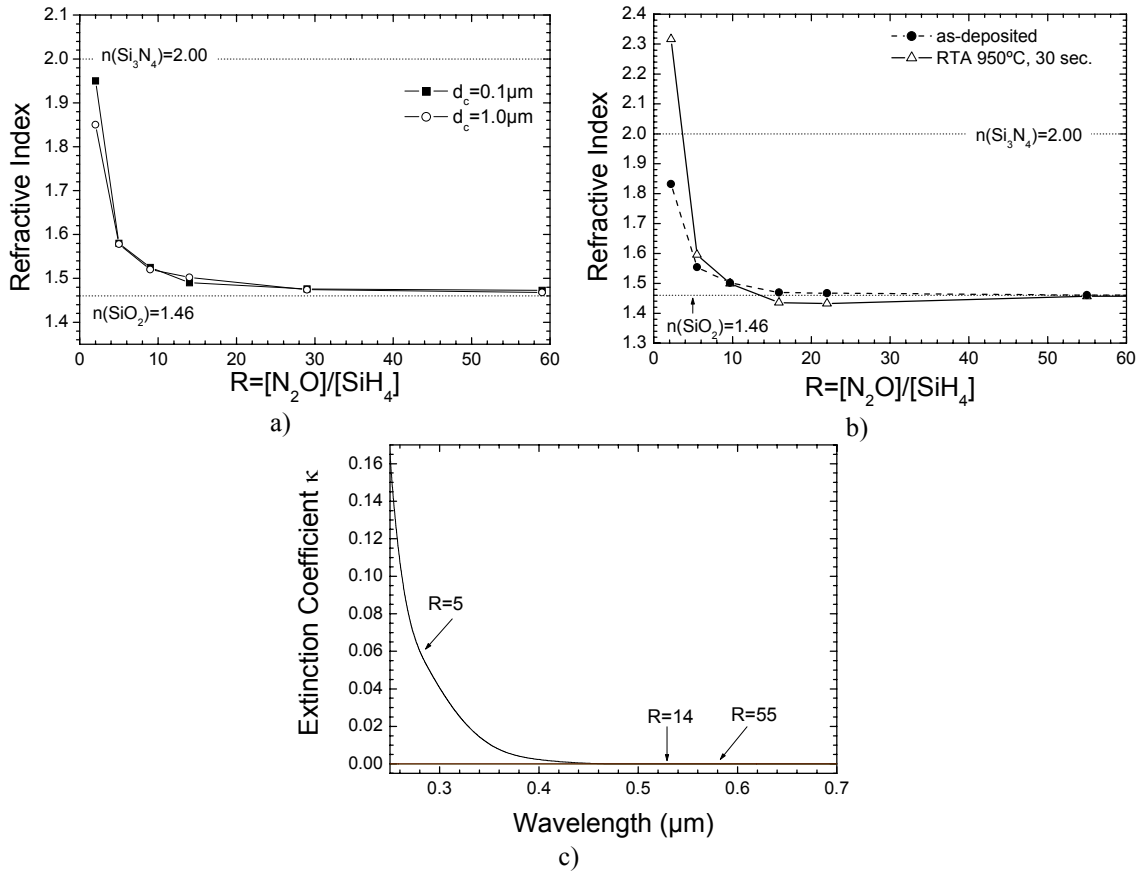

Fig 3.17: Optical properties of the SiO_x measured samples: a) refractive index as a function of the precursor's ratio for two different SiO_x thicknesses. b) Refractive index difference before and after RTA for a 1µm thick sample. c) Extinction coefficient vs. wavelength for three as-deposited samples.

Fig 3.18: Effects of the excessive mechanical stress over silicon-based multilayer structures.

Then, an exhaustive study of the mechanical stresses on the deposited layers was requested in order to obtain ARROW waveguides. Among the different models for explaining the stress during the deposition process, we have slightly modified the one

depicted in **[19]** being the scheme shown in fig. 3.19. As a rule, each material has unique mechanical properties with different behavior as the external conditions are varied (i.e., a temperature increase). Under this statement, it could be said that an isolated homogeneous, linear and isotropic material is not stressed, since it could vary its properties without any restriction at the boundaries. Problem arises when two or more layers are stacked. In this case, there exists a restriction at the interface: the fact that both layers must behave together under the influence of external perturbation causes the stress on the layers (also called bimetal effect). Consider each layer as a spring with known properties. If two springs are placed together, but there is no interaction between them, we have the situation presented in draws a1 and b1 on fig. 3.19. Now, if there exists a boundary layer and both springs are forced to have the same dimensions, opposite forces appear on both layers, forcing the substrate and the layer to expand or to shrink, depending on its initial conditions.

From the pictures 3.19 a2 and b2, it can be seen that tensile forces developed in one spring are compensated by compressive forces on the other spring. However, since both had different initial dimensions, there also exist a uncompensated bending moment that is balanced by bending the whole structure. Thus, films containing internal tensile stresses bend the substrate concavely upward (3.19a). In a similar fashion, films with compressive stresses are obtained in those layers that tend to be initially more expanded that the substrate (3.19b), which bend the substrate convexly outward.

In a standard spring, if the maximum elongation is not exceed (hook's limit), it can recover its initial size. With two different layers, the situation is analogous: if the layer is removed, the substrate recovers its initial mechanical properties. The question arises on the fact that it is known what happens to a spring when the hook's limit is exceeded, but extrapolation of this result to films is unclear. Moreover, hook's limit only comprises maximum elongation, but its minimum length is given by the spring's size. As it was shown in fig 3.19, both tensile and compressive residual stresses could result in a layer cracking. Seeing how the structure has cracked, it is possible to know how the stresses were. In picture 3.20 two opposite cracking effects can be seen. If the tensile stress is too high (fig. 3.20a), layer suffers from fracture. On the contrary,

compressive stress (fig. 3.20b) causes film wrinkling and local loss adhesion to the substrate.

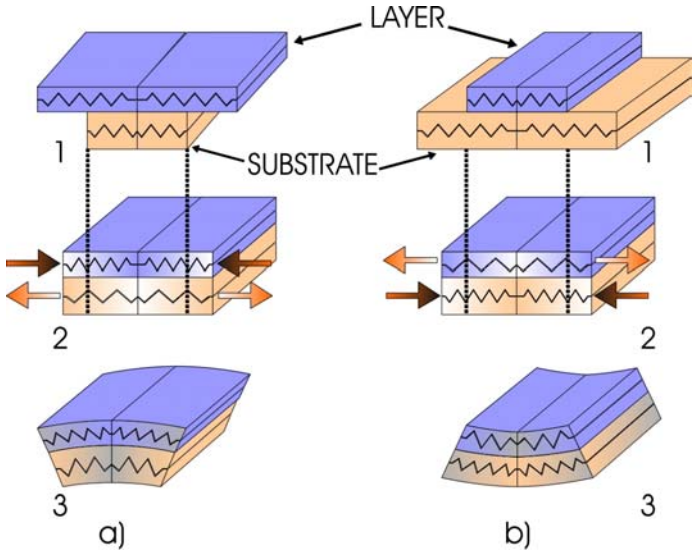

Fig 3.19: Mechanical stress due to different mechanical properties that lead to a) residual tensile (concave) bending at the layer, b) residual compressive (convex) bending at the layer.

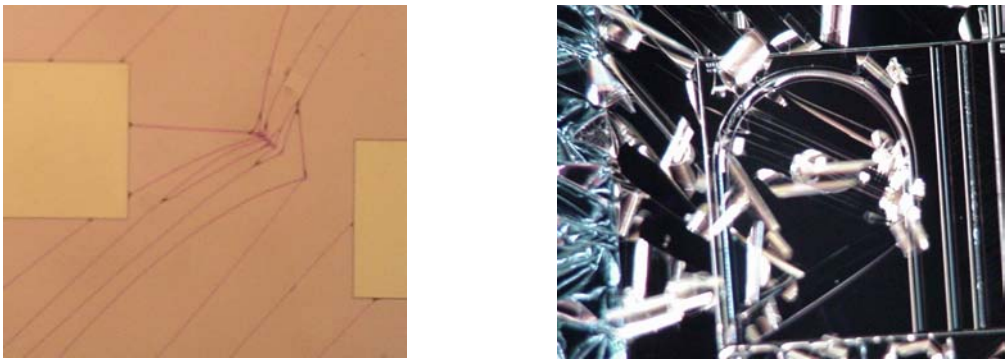

a) **b)**

Fig 3.20: a) Fracture due to a excessive tensile stress. b) Wrinkling and loss film adhesion due to excessive compressive stress.

If cracking has not been produced, mechanical stress of the oxide films can be determined by measuring the strain (change in curvature) produced in the substrate by the deposited layer. Wafer curvature before and after deposition is measured using the optically levered laser measuring system shown in fig. 3.21. It consists on a visible red laser (633nm, 1.5mWatt) aligned with the sample to be measured. After reflection at its surface, the beam is redirected towards the measuring stage. Reasons why using M3 and M4 mirrors are understood by means of the radius of curvature (R_a),

$$R_a = 2\,L\,\frac{\Delta X}{\Delta Y} \tag{3.8}$$

Displacing the sample a given distance ΔX causes a spot translation ΔY at the measuring stage, being L the total length covered by the beam after reflection on the sample surface. Thence, if L increases, the displacement will also increase and its measurement will be simpler and preciser. R_a sign is chosen, by convention, negative for convex samples (compressive film stress) and positive for concave samples (tensile film stress). During deposition, wafers are processed at a given temperature. Thence changes in the layer curvature, as a function of temperature should also be studied. Placing the wafer on a furnace with a small window on its front, by which laser reaches the wafer surface, stress measurements can be performed. Temperature is increased by ways of an electrical resistance placed on the wafer holder. It is known that heating silicon wafers in an oxidant atmosphere, even at low temperatures, causes a surface oxidation (actually, all wafers have a native silicon oxide with a thickness around 50Å caused by the ambient atmosphere). Moreover, since low temperature-deposited oxides (<350ºC) are under study, small temperature changes under oxidant atmosphere causes high variations of its structure. For that reason, the furnace has an inert gas laminar flow during all the thermal measurement process.

Once the strain of each wafer is determined, its stress may be calculated if the elastic limit has not been exceeded. Applying Hook's law, it is possible to obtain the so-called Stoney's equation **[19],** which reads:

$$\sigma_{ox} = \frac{E_{sub}}{6(1-\nu_{sub})}\,\frac{D^2}{d}\,\frac{1}{R_a} \tag{3.9}$$

In this equation, D and d are the thickness of the substrate and film, respectively, while E_{sub} and ν_{sub} stands for the Young's modulus and Poisson's ratio of the substrate, respectively. The condition d<<D and an isotropic distribution of the stress in the film cross section has been considered.

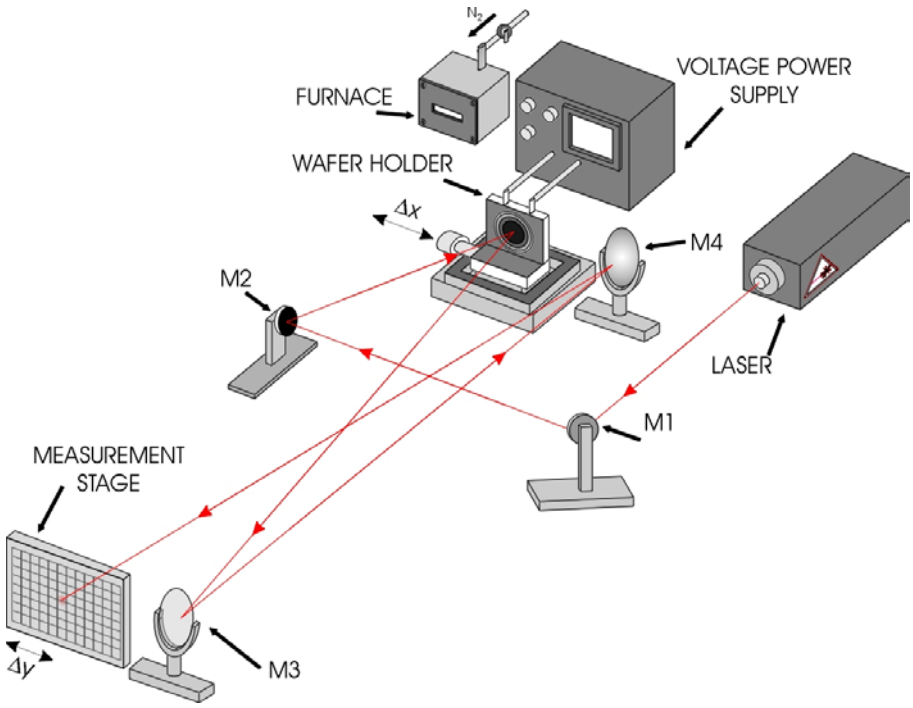

Fig 3.21: Levered laser mechanical stress measuring system. For a given sample displacement, the spot variation on the measuring stage allows determining the curvature radius and the mechanical stress. The furnace allows temperature cycles to study the stress variation against temperature.

As it was previously mentioned, films obtained at a given temperature suffer a certain stress when they are cooled down to a lower temperature, since the mechanical coefficients of the substrate and the layer are different. Since ARROW waveguides are multilayered structures, they have to stand several heating/cooling cycles. Hence, thermal effects probably provide with important contributions to total film stress. The total stress then will be be given by

$$\sigma_{ox} = \sigma_i + \sigma_{th} \tag{3.10}$$

where σ_i is the so called intrinsic stress in which the composition and structural layer properties are involved, and depends on the deposition conditions, and σ_{th} is a thermal component, which is a direct result of the different thermal expansion coefficients between the layers and can be written as

$$\sigma_{th} = \left(\alpha_{subst} - \alpha_f\right)\frac{E_f}{1-\nu_f}\left(T - T_d\right) \tag{3.11}$$

where α_{subst} and α_f are the thermal expansion coefficients of the substrate and the film, respectively, E_f and ν_f stands for the Young's modulus and Poisson's ratio of the film, T_d is the deposition temperature and T is the stress measuring temperature (usually room temperature).

The behavior of the mechanical stress as a function of the precursor ratio, before and after RTA can be seen in fig. 3.22. The so-called biaxial elastic constant (E_{sub} / 1-ν_{sub}) has been considered to be 180.5 GPa for (100) oriented Si during all mechanical stress calculations, in concordance with **[20]**. As previously mentioned, the reasons why extend our study to RTA annealed samples is to analyze the variation of the optical properties of the layers after the effusion of the impurities.

For the as-deposited films, all samples presented a negative (compressive) stress value when viewed from the oxide side. In these layers, a linear increase in absolute value of the total stress with R is observed. This behaviour can be explained due to a decrease of the elastic constants of the film **[21]**. However, if samples are RTA-annealed at 950ºC for 30 seconds in N_2 atmosphere, a broken line is obtained. To understand this behavior, layers were analyzed by Fourier-Transformed Infra-Red spectroscopy (FTIR) using a Perkin-Elmer Model 2000 spectrophotometer with a 4cm^{-1} resolution.

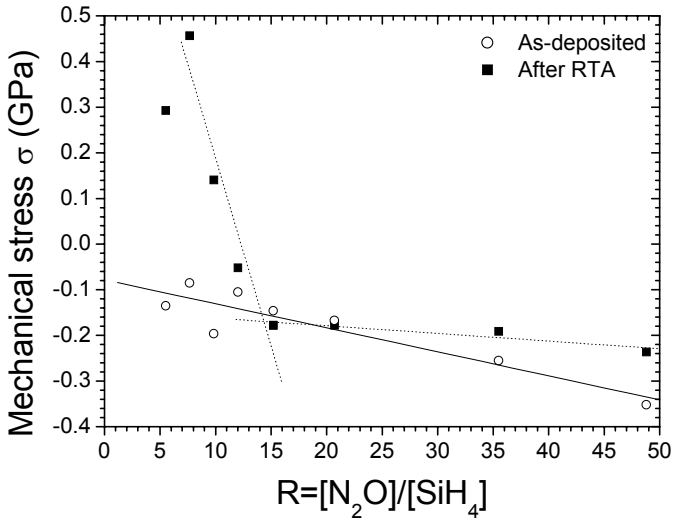

Fig 3.22: Measured mechanical stresses for as-deposited and after RTA.

As-deposited and after RTA-annealing FTIR spectra for obtained layers are shown in fig. 3.23, together with the spectrum of a thermally grown silicon oxide. It can be seen that as-deposited spectra layers with R≥20.7 are very similar to that of the SiO_2, this point is confirmed by the parity of both refractive index values observed in fig. 3.17. Actually, high R PECVD-deposited silicon oxide layers could be considered as nearly stoichiometric. There exists, however, a clear variation on the transmission spectra as R decreases. Firstly, the intensity of the Si-O-Si bending peak (located at 826cm^{-1}) gradually decreases, disappearing completely for R=5.5. On the other hand, for R=15.2 it appears a new absorption band at around 890cm^{-1}. As R decreases, this peak shifts towards a lower wavenumber and its intensity increases. Simultaneously, the Si-O-Si stretching bond band (located at 1070cm^{-1}) also shifts towards a lower wavenumber. All the previous observations can be summarized as follows: For the as-deposited films, a sort of complementarity effect exist between Si-O and Si-H contents. When R increases, an increase of the oxygen content, together with a decrease of the bonded hydrogen is observed (2200cm^{-1}). This is a direct consequence of the chemical reaction that takes place during deposition. In this process, the increase of O-species activated by electron impact dissociation leads to an efficient passivation of the Si atoms by the strongly electronegative oxygen atoms that avoid the Si-H bond formation. Finally, FTIR spectrum of the high R as-deposited layer exhibits a small band located at 936cm^{-1} and a wide band in the range 3300-3600cm^{-1}. Both bands are indicative of the presence of Si-OH bonds **[22]**.

Fig. 3.23b shows the spectra of the same samples after RTA annealing. For low R's, the absence of Si-H related peaks (located at 2200cm^{-1}) confirm that bonded hydrogen content is below the system detection limit. Thence, the hydrogen must have been desorbed from the layer during RTA, causing a film densification and shrinkage, which gives as a result the previously observed increase of the refractive index and the mechanical stress variation for low R values. When the precursor ratio is high enough so as to inhibit the hydrogen bonds due to the oxygen presence, it could be thought that this effusion no longer takes place, but it has to be considered that there also is hydrogen, in the form of Si-OH bonds, that are diffused away from the layer during

annealing. Although these two types of bonds have different properties, yet no justification has been given to the fact that high R films do not suffer the same huge change in its mechanical stress.

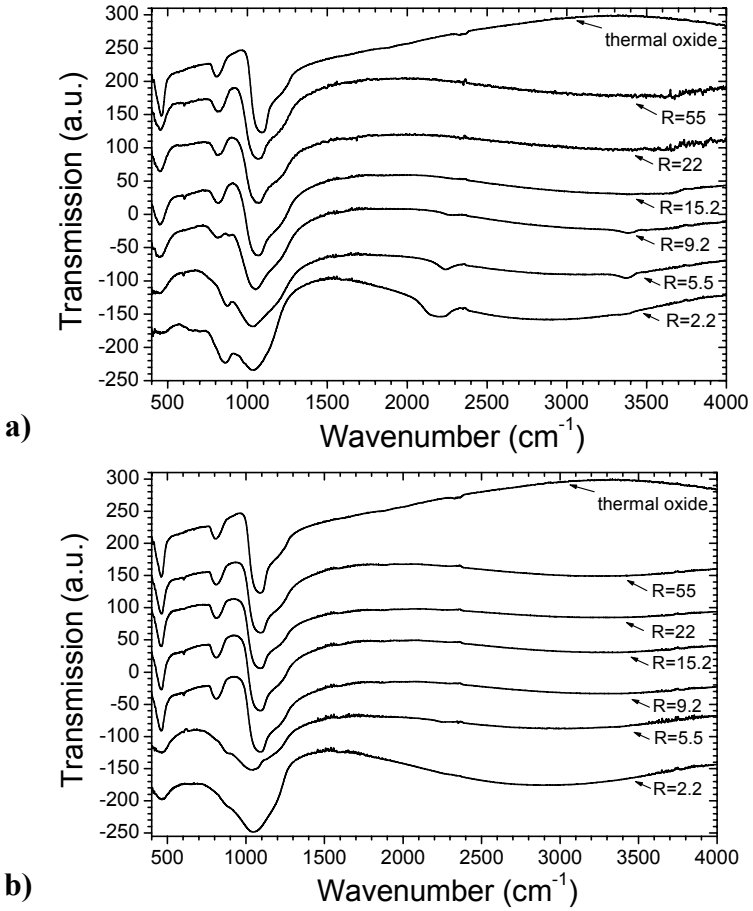

Fig. 3.23: Transmission spectra for different gas flow ratio values: a) as-deposited samples, b) RTA annealed samples.

To analyze the water-related bonds effects on the overall structure, thermal cycles up to 300ºC followed by RTA on layers of R=5.5 and R=20.7 deposited at temperatures ranging from 200ºC to 350ºC have been done.

The evolution of the films stress during the first two thermal cycles for a sample deposited at T_d=200ºC and R=20.7 can be seen in fig. 3.24. During the first cycle the stress exhibits a large hysteresis (which is defined as the stress values difference during the cooling and the heating processes, at a fixed temperature of 50ºC). On heating above 100ºC the film contracts and the substrate curvature decreases till it is

inverted and tensile stress values are obtained (concave structure). On cooling, an elastic behavior is observed and the stress remains positive. Successive thermal cycles lead to disappearing of the hysteresis and reaching a saturation value for this magnitude. Fig. 3.25 shows the results for a sample deposited at 200ºC and R=5.5. A quite different behavior is observed as compared with samples deposited at R=20.7. Even during the first cycle little hysteresis is present and the stress remains negative for successive cycles.

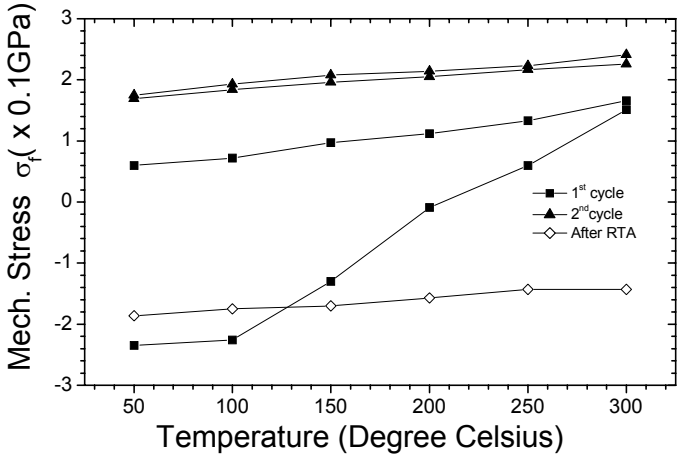

Fig. 3.24. Stress dependence with temperature for samples deposited at R = 20. 7 and T_d = 200 ºC.

After RTA, a drastic inversion of the film curvature is obtained, from convex to concave for R=5.5 and from concave to convex for R=20.7.

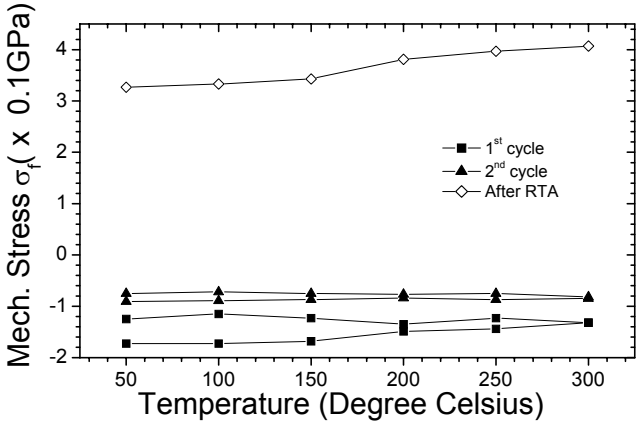

Fig. 3.25. Stress as a function of temperature during thermal cycles for layers obtained at R = 5.5 and T_d = 200 ºC.